Study of the electron structure of single crystals of terbium-yttrium alloys by the positron annihilation technique

V. P. Komlev, V. I. Kudinov, S. A. Nikitin, Yu. V. Obukhov, V. P. Posyado, and Yu. V. Funtikov

Institute of Theoretical and Experimental Physics

The electron structure of $Tb_{1-x}Y_x$ single crystals is investigated by measuring the angular distribution of the annihilation photons. An alteration of the Fermi surface, for yttrium concentrations $x < 0.4$, is revealed by the changes in the characteristic angular-distribution-function features related to the shape of the electron-momentum distribution function. The contributions of the s- and d-electrons to the valence band are estimated. It is shown that the change in the wave vector of the helicoidal magnetic structure, which occurs on alloying terbium and yttrium, depends on the change in the thickness of the "ribbon" in the hole Fermi surface.

INTRODUCTION

In alloys of terbium with yttrium $Tb_{1-x}Y_x$, which have below the Néel point an antiferromagnetic helical structure, a sharp change is observed in the magnetic, magnetostrictive, and electrical properties functions of the yttrium concentration near the value[1,2] $x \sim 0.4$. This anomaly cannot be caused by structural transformations, since the alloys are solid solutions whose hexagonal crystal lattice changes very little on melting.[3] On the basis of a theoretically established relationship between magnetic ordering and the topology of the Fermi surface,[4] it had been proposed[1] that in the region of values of $x \sim 0.4$ an electronic transition takes place in these alloys and is connected with a change in the topology of the Fermi surface.

The use of traditional methods of experimentally investigating the Fermi surface of alloys of the rare earth metals (REM) is made difficult by the strong scattering of the conduction electrons by magnetic inhomogeneities, which takes place at temperatures below the Néel point down[5] to 4.2 K. Therefore in this study the angular distribution of annihilation photons (ADAP) emitted following two-photon positron annihilation is measured to investigate the electronic structure of $Tb_{1-x}Y_x$ alloys.

EXPERIMENT

The technique of carrying out the experiment is described in detail in Ref. 6. The measurements were carried out on equipment having a long-slit geometry with an angular resolution 0.4 mrad. The radioactive isotope Cu^{64} with an activity of 300 mCi served as the positron source. The geometry of the experiments is shown in Fig. 1. The counting of photons passing through collimators K_1 and K_2 was accomplished with two scintillation detectors, D_1 and D_2 with NaI(Tl) crystals, which were placed along the X axis. The Y axis is perpendicular to the plane of the figure. The Z axis is vertical. In this system of coordinates the unit measures the number of coincident annihilation photons picked up by the detectors as a function of the divergence angle, $N(\theta)$. The momentum component p_z of the annihilation electron-positron pair is then given by the relationship[7]

$$p_z(\theta) = m_0 c\theta, \tag{1}$$

where m_0 is the electron rest mass and c is the velocity of light. Since at the instant of annihilation the positron is thermalized, p_z is determined only by the electron momentum, that is, ADAP reflects the characteristic features of the electron-momentum distribution in the substances investigated.

The technique of preparing single-crystal $Tb_{1-x}Y_x$ alloys and the determination of the content of metallic and gaseous impurities are considered in Ref. 8. Because of the low impurity content, of the insignificant and monotonic change in grain size and disorientation angles, and of the absence of phase secretions, it is possible to neglect the effect of structural defects on the shape of the Fermi surface.

The alloy samples were single-crystal disks with a diameter of 8 to 10 mm and a thickness of 3 to 4 mm. During the measurements they were arranged so that the disk axis coincided with the Z axis of the unit. Since the momentum distribution is anisotropic in $Tb_{1-x}Y_x$ alloys, two series of single-crystal samples were investigated. In the first series the crystal c [0001] axis was in the plane of the disk, with $p_z \perp c$. In the second series the crystal axis coincided with the disk axis and $p_z \| c$. For convenience, the experimental parameters of ADAP and the values calculated from these data will be designated by the indexes $\perp$ and $\|$ respectively for each series. The error in determining the angular orientation of the samples with respect to the axis of the recording system did not exceed 2°.
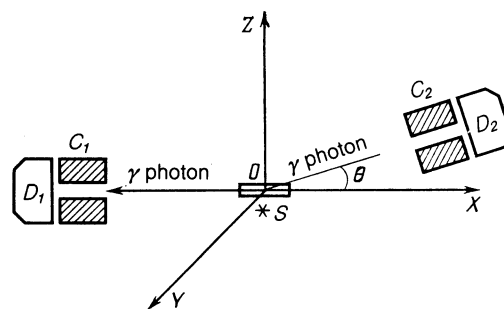
The experimental results, which were obtained for the

FIG. 1. Experimental geometry: C_1 and C_2 are collimators, D_1 and D_2 are scintillation detectors; O is the sample under study; S is the positron source. Left and right—immobile and mobile arms of the device.
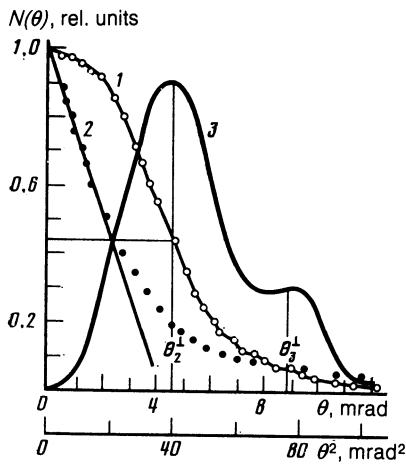
0038-5646/87/051050-04$04.00

N(θ), rel. units

FIG. 2. Distribution of the number of coincidence counts as a function of the angle θ for the alloy $Tb_{0.63}Y_{0.37}$ ($p_z \perp c$) 1—experimental curve; 2—calculated $N(\theta^2)$ dependence; 3—calculated dependence of the modulus of the derivative $|dN/d\theta|$ as a function of the angle θ.

alloy $Tb_{0.63}Y_{0.37}$, are presented in Figs. 2 and 3 as an example. The quadratic abscissa scale is used to show the angle regions in which the ADAP has the shape of a parabola. The derivative modulus $|dN/d\theta|$ was calculated as a function of the angle from these data. Values of the angles θ_1, θ_2, and θ_3, which correspond to extrema of this dependence, will be used in discussion of the results. The experimental curves are similar in form for $Tb_{1-x}Y_x$ alloys of other compositions, but the angles θ_1 to θ_3 and the areas under various parts of the ADAP graphs are different. A total of 12 samples was investigated. Each experiment lasted 10 to 12 hours and yielded a total of 5×10^5 events in each distribution.

DISCUSSION OF RESULTS

The experimental data can be interpreted on the basis of the results of theoretical ADAP calculations based on the independent-particle model and on the relativistic augmented plane wave (APW) method.[9] For $N(\theta) = N(p_z/m_0c)$ the following expression was obtained:
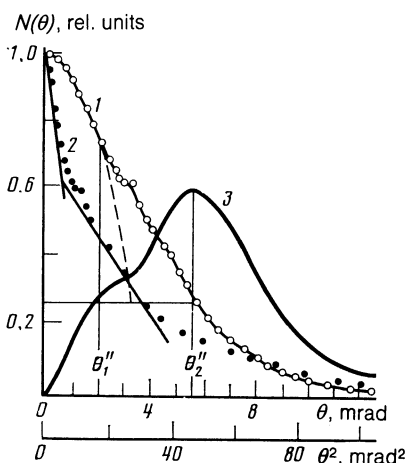
N(θ), rel. units

FIG. 3. Distribution of the number of coincidence counts as a function of the angle θ for the alloy $Tb_{0.63}Y_{0.37}$ ($p_z \| c$): 1—experimental curve; 2—calculated $N(\theta^2)$ dependence; 3—calculated dependence of the modulus of the derivative $|dN/d\theta|$ as a function of the angle θ.

$$N(p_z) = A(p_z)F(p_z), \tag{2}$$

where $A(p_z)$ is the number of occupied electron states in a plane cross section of the Fermi surface in a periodic zone system at a distance p_z from the origin in momentum space; $F(p_z)$ is the probability that an electron with momentum p_z annihilates with a thermalized positron. $F(p_z)$ varies little with p_z within the Brillouin zone, and decreases near its boundary. In the investigated alloys the crystal lattice parameters monotonically increase with increasing yttrium content. The ensuing change $\Delta\theta$ in the angle corresponding to the boundary of the Brillouin zone does not exceed 0.03 mrad in $Tb_{1-x}Y_x$ alloys, which is significantly less than the uncertainty $\Delta\theta_T \approx 0.35$ mrad caused by the thermal motion of the positron.[10] On the assumption that the function $F(p_z)$ is the same for all alloys in the $Tb_{1-x}Y_x$ system, the changes of the ADAP can be used to track changes of the areas of the Fermi-surface cross sections perpendicular to p_z.

The linear dependence of N on θ^2 at $p_z \perp c$ (Fig. 2) can be explained by the fact that a group of valence electrons participates mainly in the annihilation processes at small angles ($\theta_2 \perp \approx 5$ mrad). In this case the Fermi surface has the shape of a sphere. In the approximation in which the wave function $F(p_z)$ is the same for all alloys of the $Tb_{1-x}Y_x$ system, with changes being constant, we get from (2) a simple relation between the ADAP and the electron momentum p_z (Ref. 11):

$$N(\theta) \propto (p_F^2 - p_z^2), \tag{3}$$

where p_F is the Fermi momentum. Consequently the $N(\theta)$ plot has in this the shape of a parabola, while the angle $\theta_2^{\perp}$ (Fig. 2) should correspond to the Fermi momentum $p_F^{\perp}$ of the conduction electrons.

To estimate the contributions to positron annihilation with valence electrons (S_n) and with core electrons (S_0) the area under the $N(\theta)$ curve was divided into corresponding parts.[12] S_n was found to be the area bounded by the curve $N(\theta)$, the ordinate axis and a straight line parallel to the abscissa and passing through the point having the abscissa θ_2 on the $N(\theta)$ curve (Fig. 2 and Fig. 3). S_0 was found as the difference between the total area under the $N(\theta)$ curve and S_n. The concentration dependence of the ratio S_n''/S_0'' is presented in Fig. 4 (curve 4).

According to our experimental data the ratio $S_n^{\perp}/S_0^{\perp}$ as well as the value of $\theta_2^{\perp}$ does not depend on the yttrium content in the alloys ($S_n^{\perp}/S_0^{\perp} = 0.61 \pm 0.04$; $\theta_2^{\perp} \approx 4.5$ mrad). These data indicate that the cross-section areas of the Fermi surface perpendicular to the base plane remains practically constant when terbium is alloyed with yttrium.

The number k of conduction electrons per atom can be estimated by using a relation which is correct for free electrons, and takes the following form[13] for an hcp structure:

$$k = \frac{3^{1/2}}{4}\left(\frac{c_0}{a_0}\right)a_0^3 \cdot \frac{8\pi}{3h^3}p_F^3, \tag{4}$$

where h is Planck's constant; a_0 and c_0 are lattice parameters. By using the known values of a_0 and c_0 for $Tb_{1-x}Y_x$ alloys[3], Eq. (1), and the experimental values of $\theta_2^{\perp}$, we estimated the number of conduction electrons per atom, $k^{\perp}$ = 1.7–2.0, when the electron momentum lies in the basal plane.
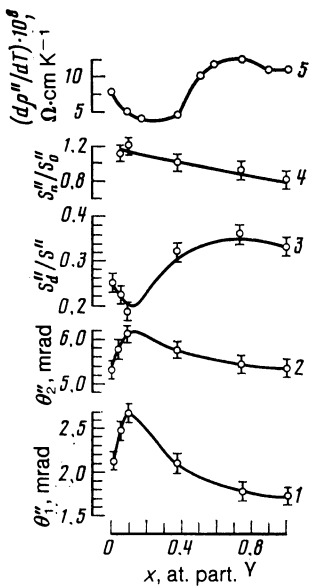
FIG. 4. Experimental dependences of the ADAP parameters in the alloys $Tb_{1-x}Y_x$ ($p_z \| c$) as a function of yttrium concentration: 1—θ_1''; 2—θ_2''; 3—s_d''/s''; 4—S_n''/S_0''; 5—dp''/dT [5].

It is known that the outer electron shell of yttrium atoms has a $4d\,5s^2$ configuration, while that for terbium is $5d\,6s^2$ configuration. In the metallic state the zone III and "trunk" of the anisotropic hole Fermi-surface is made up mainly of s-bands[14]. The values of $S_n^\perp/S_0^\perp$ and $k^\perp$ that we obtained show that the main contribution to annihilation, for directions lying in the base plane ($p_z \perp c$) is due to the s-electrons. It follows from our data that this contribution and "trunk" of the Fermi surface in zone III changes little when terbium with yttrium are alloyed.

The ADAP curve for $p_z \| c$ can be described by a superposition of two parabolas (Fig. 3). Apparently this indicates that s- and d-electrons participate in annihilation processes. This conclusion agrees with theoretical calculations (Ref. 14), according to which the Fermi-surface cross sections perpendicular to the hexagonal axis c in zone IV are filled to a significant degree by d-bands. On the assumption that the angles θ_2'' found experimentally from the ADAP curves correspond to a Fermi-momentum $p_F'' = m_0 c\,\theta_2''$, we estimated from Eq. (4) the value of k'' and the total number of s- and d-electrons per atom. The value of k'' in the alloys $Tb_{0.95}Y_{0.05}$ and $Tb_{0.91}Y_{0.09}$ exceeds three, and then decreases to $k''\approx 2.7$ with increasing yttrium content.

The maximum modulus of the derivative $|dN/d\theta|$ near $\theta_1 \sim 2$ mrad, and the "hump" on the ADAP curve near 3 mrad for $p_z \| c$, are typical characteristic features of heavy rare-earth metals and yttrium (Ref. 10), and also, according to our data, of $Tb_{1-x}Y_x$ alloys. As theoretical calculations of ADAP (Ref. 9) have shown, these characteristic features are associated with the fact that the function $A(p_z)$, which characterizes the cross-section area of the Fermi surface, has a minimum at momentum values p_z corresponding to the angle $\theta_1 \approx 2$ mrad. This minimum is the result of the crowding-out of the electron states during formation, in the hole Fermi-surface, of a "ribbon" that connects the symmetry points L and H at the boundary of zones III and IV (Ref. 13). The thickness of this "ribbon" is equal to the modulus of the wave vector of the helicoidal magnetic structure (Ref.

13), $f = 2\pi/L$, where $L = \pi c_0/\alpha$ is the period of the structure (α is the helicoid angle). The axis of the helicoid coincides with the hexagonal axis c of the crystal lattice of the $Tb_{1-x}Y_x$ alloys (Ref. 15). In momentum space the modulus of the vector $\mathbf{f}$ corresponds to $\hbar f = 2\pi(\alpha/c_0)$. In this same space, the angle θ_1 determines the position of the "ribbon" at boundary of zone III and IV.

The change in the wave vector $\hbar\mathbf{f}$ of a magnetic helicoidal structure on going from alloys with a high yttrium content ($x > 0.9$) to alloys with a low yttrium content is, in angle measure,

$$\Delta(\hbar f) = \frac{2}{c_0}\hbar\frac{1}{m_0 c}(\alpha_Y - \alpha),\qquad (5)$$

α_y and α are the initial rotation angles of the helicoid at the Néel point, respectively, for alloys with high and low yttrium content.

According to neutron-diffraction measurements[15] the helicoid angle monotonically decreases in $Tb_{1-x}Y_x$ alloys with decreasing yttrium content, with $\alpha_y \approx 50°$ for alloys with a low yttrium content and $\alpha \approx 27°$ for the $Tb_{0.9}Y_{0.09}$ alloy. On substituting these values and also the lattice constant $c_0 \approx 5.78$ Å in Eq. (5), we obtain $\Delta(\hbar f) \approx 0.54$ mrad, which corresponds in order of magnitude to the difference

$$\Delta\theta_1'' = (\theta_1'')_{max} - (\theta_1'')_{min} \approx 0.9 \text{ mrad},$$

which we determined by investigating $Tb_{1-x}Y_x$ alloys (Fig. 4, curve 1). This indicates that the increase of θ_1'' with decreasing yttrium content in the alloys is caused by a decrease of the angle and wave vector of the helicoid. On the other hand, the increase of the angle θ_1'', which determines the position of the "ribbon" in momentum space, is uniquely connected with the decreasing thickness of the "ribbon" between points L and H of the hole Fermi-surface with decreasing yttrium content in the alloys. A particularly abrupt change in the value of θ_1'' and $\hbar f$ is observed in the region of yttrium concentration $x < 0.4$ (Fig. 4, curve 1). Thus our experimental data agree with the theoretical conclusions of Dayaloshinskiĭ (Ref. 4) that the wave vectors of magnetic helical structures in rare-earth metals are determined by the extremal diameters of the Fermi surface.

With further decrease in the yttrium concentration ($x < 0.09$) a sharp decrease occurs in the values of θ_1'' and θ_2'' (Fig. 4, curves 1 and 2) by approximately the same amount. This decrease is explained by an additional restructuring of the Fermi surface. Apparently the restructuring is connected with a decrease in the number of occupied electron states at the point M, since calculations show (Refs. 13, 16, 17) that the structure of terbium has there at this point a hole Fermi-surface "shoulder" which is absent in yttrium.

For a quantitative estimate of the ratio of annihilation probabilities in the two selected groups of s- and d-electrons, we turn to the experimental results presented for $p_z \| c$ in Fig. 3. The area S_n'' is proportional to the total number of states occupied by conduction electrons. The area S_s'', which is bounded by an upper parabola (dotted curve in Fig. 3), corresponds to the relative number of states occupied by s-electrons. Consequently the area $S_d'' = S_n'' - S_s''$ characterizes the number of states occupied by d-electrons. The concentration dependence of the area ratio S_d''/S_s'' is presented in Fig. 4 (curve 3). The change in value of S_d''/S_s'' as a function

of the yttrium content in the alloys can be attributed to a redistribution of conduction electrons among the s- and d-groups. This change can be compared with previously obtained results of a study of the electrical properties of the alloys.[5] The following expression is correct for the temperature coefficient of the electrical conductivity along the hexagonal axis in the paramagnetic state

$$d\rho''/dT = B\left[\left(\tau_{ph}\int_{E_F} dS''\right)^{-1} + \left(\tau_e\int_{E_F} dS''\right)^{-1}\right], \qquad (6)$$

where B is a constant; the integral indicates the sum of Fermi-surface projections on a plane perpendicular to the c axis; τ_{ph} and τ_e are relaxation times respectively via scattering on phonons and via scattering in multi-electron collisions.

Estimates show that the change in relaxation times in $Tb_{1-x}Y_x$ alloys does not exceed 10%. Consequently the steep change of $d\rho''/dt$ with concentration (Fig. 4, curve 5) indicates an increase in the value of the corresponding integral at an yttrium content in the alloys $x < 0.4$. This is in agreement with the decrease in the number of occupied d-electron states at $x < 0.4$, as obtained from an analysis of the concentration dependence of the ratio S''_d/S''_s. The results of a zone structure calculation (Ref. 17) also show that in terbium the number of occupied electron states in zone IV decreases as a result of the appearance of a "shoulder" M at the hole Fermi surface.

The presence of additional maxima, at angle values θ_3, on the plots the modulus of the derivative $|dN/d\theta|$ vs the angle θ for the basal plane (Fig. 2), and their absence for the direction $p_z \| c$ (Fig. 3), shows that annihilation with electrons on the ion core has an anisotropic character. One of the possible reasons of the anisotropy may be the contribution from annihilation with $4f$-electrons, which have in terbium an orbital momentum different from zero, and energy levels close to the energy of the conduction band.[18]

CONCLUSIONS

The results of this study show that the method of measuring the angular distribution of annihilation photons is effective in the study of the electron structure of rare-earth-metal alloys. Studies of $Tb_{1-x}Y_x$ alloys conducted by this method showed that the characteristics of conduction electrons display a strong anisotropy, that is, a dependence of these characteristics on the direction of the electron momentum in the crystal lattice. It was concluded that in $Tb_{1-x}Y_x$ alloys, at yttrium concentrations $x < 0.4$, a substantial restructuring of the Fermi surface takes place, from an "yttrium" type ("ribbon," absence of a shoulder M in the hole Fermi-surface) to a "terbium" type (slight "ribbon", the presence of a shoulder M). Two groups of conduction electrons were singled out: s and d electrons. On alloying terbium with yttrium, a redistribution of the number of s and d electrons takes place over the energy bands. This redistribution has a definite effect on the restructuring of the Fermi surface of $Tb_{1-x}Y_x$ alloys.

[1]K. P. Belov, S. A. Nikitin, N. A. Sheludko *et al.*, Zh. Eksp. Teor. Fiz. **73**, 270 (1977) [Sov. Phys. JETP **46**, 140 (1977)].

[2]S. A. Nikitin, A. S. Andreenko, V. P. Posyado, and G. E. Chuprikov, Fiz. Tverd. Tela (Leningrad) **19**, 1977 (1972) [*sic*].

[3]V. A. Funkel', Structure of Rare Earth Metals [in Russian], Metallurgiya, 1978, p. 128.

[4]I. E. Dayaloshinskiĭ, Zh. Eksp. Teor. Fiz. **47**, 336 (1984) [Sov. Phys. JETP **20**, 223 (1965)].

[5]K. P. Belov, S. A. Nikitin, V. P. Posyado, and G.E. Chuprikov, *ibid.* **71**, 2204 (1976) [**44**, 1162 (1976)].

[6]V. P. Komlev, V. I. Kudinov, Yu. V. Obukhov, and Yu. V. Funtikov, Preprint ITÉF, No. 16, 1982.

[7]V. I. Gol'danskiĭ, Physical Chemistry of the Positron and Positronium, Moscow, Nauka (Science), 1968.

[8]V. P. Posyado, M. L. Grachev, and G. E. Chuprikov, Metally (Metals), No. 3, p. 91 (1978).

[9]T. Loucks, Phys. Rev. **144**, 504 (1966).

[10]R. Williams and A. Mackintosh, Phys. Rev. **168**, 679 (1968).

[11]V. L. Sedov, Usp. Fiz. Nauk **94**, 417 (1969) [Sov. Phys. Usp. **11**, 163 (1969)].

[12]S. Szuskiewicz, Acta Phys. Polonica **A44**, 691 (1973).

[13]A. P. Cracknell and K. C. Wong, *The Fermi Surface*, Oxford, 1973, p. 350.

[14]A. Freeman, *Magnetic Properties of Rare Earth Metals*, edited by Elliott, London, Plenum Press, 1972, p. 256.

[15]H. Child, W. Kochler, E. Wollan, and J. Cable, Phys. Ref. **138**, 1655 (1965).

[16]S. Keeton and T. Loucks, Phys. Rev. **168**, 672 (1968).

[17]C. Jackson, Phys. Rev. **178**, 949 (1969).

[18]Y. Baer and J. Long, J. Appl. Phys. **50**, 7485 (1979).

Translated by S. J. Rimshaw

1053   Sov. Phys. JETP **65** (5), May 1987

Komlev *et al.*   1053